

Supporting Information for: Designing Broadband Pulsed Dynamic Nuclear Polarization Sequences in Static Solids

Nino Wili¹, Anders Bodholt Nielsen², Laura Alicia Völker¹, Lukas Schreder¹, Niels Chr. Nielsen², Gunnar Jeschke¹ and Kong Ooi Tan³

¹ *Department of Chemistry and Applied Biosciences, Laboratory of Physical Chemistry, ETH Zurich, Vladimir-Prelog-Weg 2, 8093 Zurich, Switzerland. E-mail: nino.wili@alumni.ethz.ch*

² *Interdisciplinary Nanoscience Center (iNANO) and Department of Chemistry, Aarhus University, Gustav Wieds Vej 14, DK-8000 Aarhus C, Denmark*

³ *Laboratoire des Biomolécules, LBM, Département de Chimie, École Normale Supérieure, PSL University, Sorbonne Université, CNRS, 75005 Paris, France. E-mail: kong-ooi.tan@ens.psl.eu*

Contents

S.1	Illustration of the interaction frame transformation	2
S.2	Calculation of Fourier coefficients and scaling factors for BEAM	4
S.3	Comparison of numerical and analytical computations for strongly coupled protons	13
S.4	Three-spin transitions	14
S.5	Resonator profile	15
S.6	Experimental determination of $T_{1,e}$	16
S.7	Experimental determination of $T_{1,n}$	17

S.1 Illustration of the interaction frame transformation

A central element in calculating the scaling factors a_{\mp} is the interaction frame transformation with respect to the irradiation sequence and the transformation to a cyclic frame. Here, we give a concrete example of the elements of $R^{(\text{control})}$ and $R^{(\text{eff})}$ and their relationship. We consider an XiX-DNP experiment (parameters here not chosen to represent any good DNP sequence, but for easier explanation) with $\nu_1 = 4$ MHz, $t_{p,1} = 14$ ns, $t_{p,2} = 28$ ns, and $\Omega_S/2\pi = 25$ MHz. Figure S1(a) shows the elements of the initial interaction frame transformation $R^{(\text{control})}(t)$ plotted over one period τ_m . The blue curves denote the trajectory of the normal rotating frame operator S_z . Note that $R^{(\text{control})}(0) = \mathbb{1} \neq R^{(\text{control})}(\tau_m)$, i.e. the trajectory is not cyclic with τ_m . This prohibits the straight-forward application of average Hamiltonian theory and is the reason for the subsequent transformations. Figure S1(b) shows the three-dimensional trajectory of the original S_z operator in the initial interaction frame (the three blue components in panel (a)). The trajectory of the first modulation period is marked in red. The end points of the subsequent five periods are shown as black dots in panel (b). The overall rotation from one period to the next can be described by an effective field shown in gray. This can be understood as a constant effective field, which can be removed by flipping the frame such that the effective field is along z , and then going into an interaction frame with said effective field. The result of this transformation, $R^{(\text{eff})}$, is shown in Figure S1(c) and (d). The z -axis in this new frame points along the effective field in Figure S1(b), and the effect of the overall rotation was eliminated by a counter rotation, i.e. start and end points of the trajectories are now the same. In Figure S1(c), all the coefficients are cyclic with time τ_m . A Fourier transform of the respective time-dependent coefficients directly yields the coefficients $a_{\chi z}^{(k)}$. An example script to perform these calculations in MATLAB is given below.

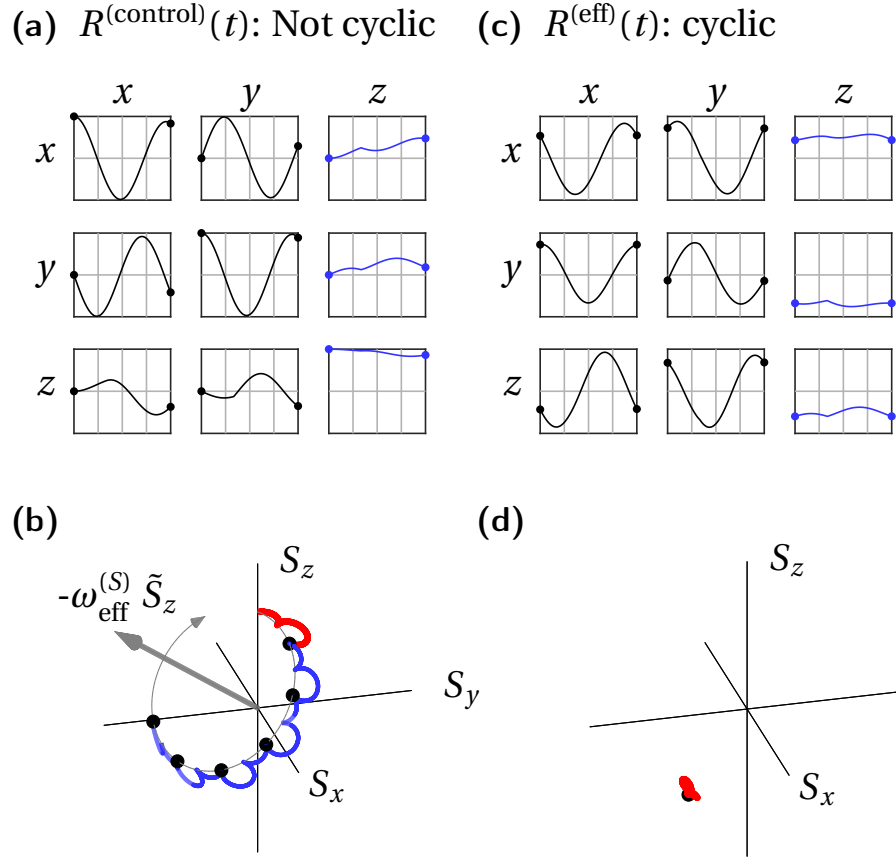


Fig. S1: Illustration for the interaction frames employed in this work, on the example of XiX-DNP (details in main text). **(a)** Illustration of the initial interaction frame transformation $R^{(\text{control})}(t)$. The individual plots show the evolution of rotation matrix elements over one period τ_m . **(b)** Three-dimensional trajectory of the original S_z operator in the initial interaction frame (the three blue components in **(a)**). The trajectory of the first modulation period is marked in red. The end points of the subsequent five periods are shown as black dots. The effective field describes the overall rotation of the sequence. **(c)** and **(d)** The same trajectory as in **(a)** and **(b)**, but in the flipped, effective (or cyclic) frame. The start and end points are the same.

S.2 Calculation of Fourier coefficients and scaling factors for BEAM

In this section, we show an example of how to calculate the effective fields and scaling factors on the example of BEAM. Although BEAM is best applied on-resonant, we include here an offset of 5 MHz for illustration. The example can be found in the file `DNPexample_BEAM.m`.

S.2.1 Build the rf-irradiation

```
1 clear, close all
2
3 % add helper functions
4 addpath(genpath('./core/'))
5
6
7 %% define sequence parameters
8 nu_I=-14.83;           % Nuclear Zeeman frequency
9 nu_1=32;               % Electron Rabi freq
10 tp1=20*1e-3;          % first pulse length in BEAM
11 tp2=(1+tp1*(nu_1-abs(nu_I)))/(abs(nu_I)+nu_1); % second pulse
    length in BEAM
12
13
14 nu1_vec = nu_1*[1 1];
15 tp_vec = [tp1 tp2];
16 phi_vec = [0 180]/180*pi; % phases of the pulses
17 dt =0.1e-4;             % time step of numerical IFT
18
19 offset = 5;
20
21 rho0_vec = [-1 0 0]';
22
23 %% build rf
24 [ rf, time ]=build_rf(tp_vec,nu1_vec,phi_vec,dt);
25
26 %plotting
27 h = figure(1);
28 clf
29 hold on
30 plot(time*1e3,real(rf),'b')
31 plot(time*1e3,imag(rf),'r')
32 xlabel('t / ns')
33 ylabel('\nu_1 / MHz')
34 axis([-1 60 -40 40])
```

35 `legend('real(rf)', 'imag(rf)', 'location', 'northeast')`

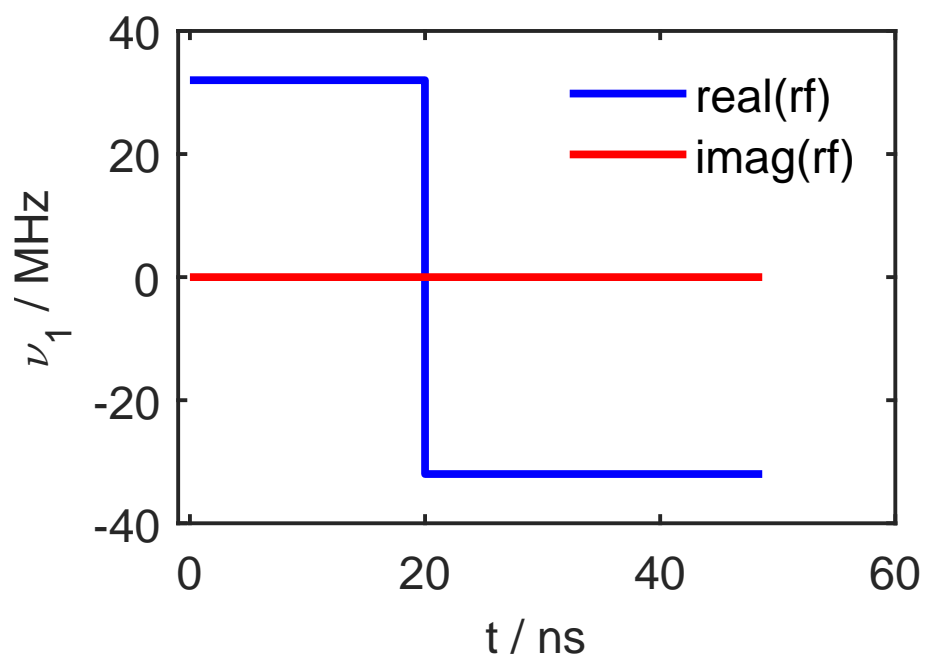


Fig. S2: rf-irradiation scheme for the BEAM simulation.

S.2.2 Calculate $R^{(\text{control})}(t)$

```
42 % generate a vector of offsets the same length as rf
43 offset=offset*ones(size(rf));
44
45 %calculate modulation frequency
46 wmod=2*pi/(time(end)+dt);
47 nu_m = wmod/2/pi;
48
49
50 % pre-allocate rotation matrices
51 R_control = zeros(3,3,numel(time));
52 R_flipped = zeros(3,3,numel(time));
53
54
55 % build array of rotation quaternions for every step
56 q_pulse = zeros(4,numel(time));
57 for it = 1:numel(time)
58     q_pulse(:,it)=quat_rf(abs(rf(it)),angle(rf(it)),offset(it),dt,'frame'
59         ) ;
60
61
62 % multiply the quaternionas step-by-step and
63 % express them as an array of rotation matrices (for plotting only at
64     this stage)
65 qtot = [1 0 0 0]';
66 q_control = zeros(4,numel(time));
67 for it=1:numel(time)
68     q_control(:,it)=qtot;
69     R_control(:, :, it) = quat2rotmat(qtot);
70     qtot = quatmult(qtot,q_pulse(:,it));
71 end
72
73
74 % Plot IF in rotating frame
75 IF_plot(time,R_control,2);
```

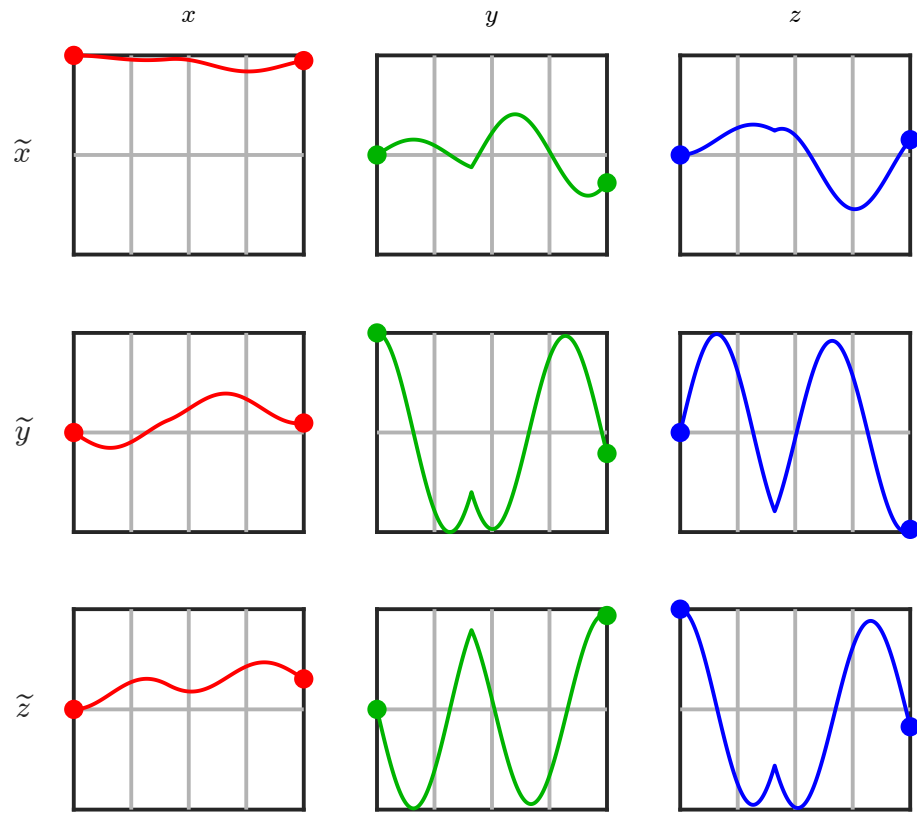


Fig. S3: Time-dependence of each element of $R^{(\text{control})}(t)$.

S.2.3 Remove the effective field from $R^{(\text{control})}(t)$, determine $R^{(\text{eff})}(t)$

```
82 %% flip each quaternion of q_control (or R_control)
83 % such that the effective field is now along the z-axis
84
85 %determine the effective field (effective flip angle and direction)
86 [z_eff,beta_eff] = quat2eff(qtot);
87
88 % determine R_flip, or the corresponding quaternion, respectively
89 % see https://doi.org/10.1063/1.5123046 for details
90 u_z = [0 0 1]';
91 q_flip = cross(z_eff,u_z);
92 qr_flip = 1+u_z'*z_eff;
93 q_flip = [qr_flip; q_flip ];
94 q_flip = q_flip/sqrt(sum(q_flip'*q_flip));
95
96 % flip all quaternions/rot-matrices
97 q_flipped= zeros(4,numel(time));
98 for it=1:numel(time)
99     q_flipped(:,it)=quatmult(q_flip,q_control(:,it));
100     R_flipped(:, :,it) = quat2rotmat(q_flipped(:,it));
101 end
102
103 %% remove the effective field from the IFT, i.e. calculate R_eff(t)
104 % determine the effective field frequency
105 w_eff = beta_eff/(time(end)+dt);
106 nu_eff = w_eff/(2*pi);
107
108 %pre-allocate rotation quaternions/matrices
109 q_eff = zeros(4,numel(time));
110 R_eff = zeros(3,3,numel(time));
111
112 % calculate R_eff(t)
113 for it=1:numel(time)
114
115     %calculate Rz(-weff*t),
116     beta = -w_eff*time(it);
117     q_z = [cos(beta/2) sin(beta/2)*[0 0 1]]';
118
119     q_eff(:,it)=quatmult(q_z,q_flipped(:,it));
120     R_eff(:, :,it) = quat2rotmat(q_eff(:,it));
121 end
122
```


123 IF_plot(time,R_eff,3);

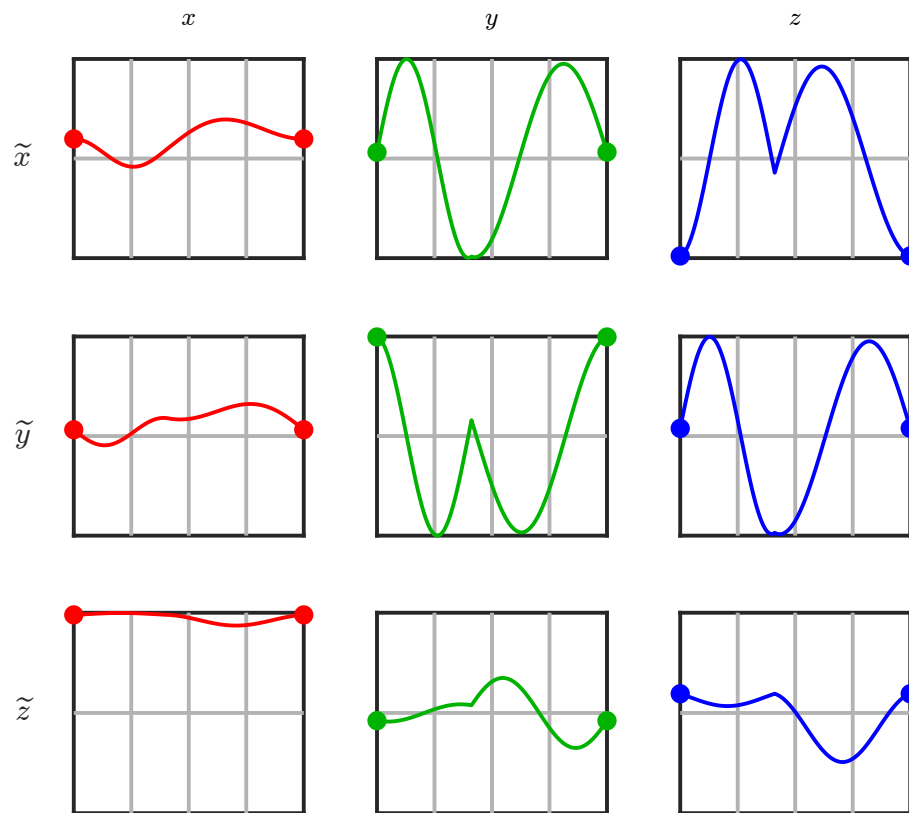


Fig. S4: Time-dependence of each element of $R^{(\text{eff})}(t)$. Note that all elements are preiodic.

S.2.4 Calculate the Fourier coefficients and scaling factors

```
128 %% calculate Fourier coefficients a^(k)
129 N=numel(time);
130 k_vec = ((0:N-1)-fix(N/2));
131 if mod(N,2)==0
132     k_vec = k_vec(2:end);
133 end
134
135 A_k = zeros(3,3,numel(k_vec));
136
137
138 % Fourier transform each element (xx,xy,xz,...zz) of R_eff(t)
139 for ii=1:3
140     for jj=1:3
141         y = squeeze(R_eff(ii,jj,:));
142         a = fftshift(fft(y))/numel(y);
143         if mod(N,2)==0
144             A_k(ii,jj,:)=a(2:end);
145         else
146             A_k(ii,jj,:)=a(1:end);
147         end
148     end
149 end
150
151
152 %extract the original z operator (should no oszillate during free
    evolution)
153 Az_k = squeeze(A_k(:,3,:));
154
155 %% extract the relevant scaling factor
156
157 [nu_eff_I,kI] = get_nu_eff_I(nu_I,nu_m);
158
159 kmax=max(k_vec);
160
161 ax = squeeze(Az_k(1,:));
162 ay = squeeze(Az_k(2,:));
163 ap = ax-1i*ay;
164 am = ax+1i*ay;
165 az = squeeze(Az_k(3,:));
166
167
```

```

168 k0 = kmax+1;
169 k = kmax+1+kI;
170 mk = kmax+1-kI;
171
172 rel_sign = sign(nu_eff*nu_eff_I);
173 if rel_sign == 1
174     a_eff= -sqrt(ap(mk)*am(k)) ;
175 else
176     a_eff= sqrt(am(mk)*ap(k)) ;
177 end
178
179 proj = z_eff'*rho0_vec;
180
181 f_pm = a_eff*proj

```

S.2.5 Compare with fully numerical calculation

```

183 %% comparison with numerical simulation
184
185 Ntheta = 31; %number of orientations
186
187 r=4.5; % e-n distance in Angstrom
188 Nrounds = 200; %number of repetitions of the DNP element
189
190 %caluclate the transfer numerically
191 [t_num,sig_num]=DNP_numerical(tp_vec,phi_vec,nul_vec,offset,nu_I,rho0_vec
    ,r,Ntheta,Nrounds);
192
193 h4=figure(4);
194 clf
195 hold on
196 plot(t_num,sig_num)
197
198 %% analytical calculation
199 %calculate the mismatch
200 delta_nu_eff = abs(nu_eff_pieewise(tp_vec,phi_vec,nul_vec,offset))-abs(
    nu_eff_I);
201
202 %calculate the anisotropy of the hf-coupling
203 natural_constants
204 T = mu0/(4*pi)*gfree*bmagn*g1H*nmagn*1/(r*1e-10)^3/planck/1e6;
205
206 %generate orientations and corresponding weights

```

```

207 theta_vec = linspace(0,pi/2,Ntheta);
208 weights=sin(theta_vec); weights=weights/sum(weights);
209
210 %preallocate results
211 t_theo = t_num(1:10:end);
212 sig_theo = zeros(1,numel(t_theo));
213
214 %loop over orientations, sum up results
215 for itheta = 1:Ntheta
216
217     theta=theta_vec(itheta);
218     B=3*sin(theta)*cos(theta)*T;
219     nu_pm = sqrt(B^2*a_eff^2/4+delta_nu_eff^2); %transfer frequency
220     transfer_amp = a_eff^2*B^2/(4*nu_pm^2); %amplitude of transfer
221
222     sig_theo = sig_theo+weights(itheta)*sign(a_eff)*proj*transfer_amp*...
223         sin(1/2*(2*pi*nu_pm)*t_theo).^2;
224 end
225 plot(t_theo,sig_theo,'o')
226
227 axis([xlim -0.1 0.8])
228 xlabel('t / \mu s')
229 ylabel('<I_z>')
230 legend('num.','theo.','location','northeast')

```

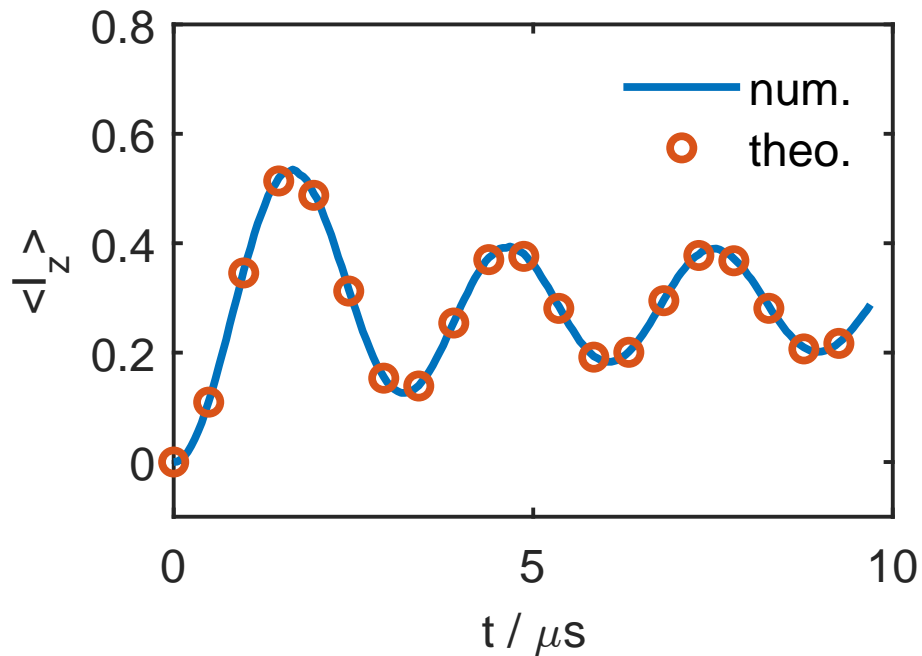


Fig. S5: Fully numerical simulation vs. effective Hamiltonian calculation.

S.3 Comparison of numerical and analytical computations for strongly coupled protons

Figure 3(b) in the main text showed a comparison of numerical and analytical computations for a proton at a distance of $r_{en} = 4.5 \text{ \AA}$. This is already quite close. Here we show what happens if one looks at protons that are even closer (2.5 \AA), see Figure S6. In this case, the hyperfine coupling is very strong. Nevertheless, the full first-order Hamiltonian (blue line) still perfectly describes the transfer. However, it is clear that only looking at the effective fields and the flip-flop terms (red) becomes more and more problematic for strong hyperfine couplings.

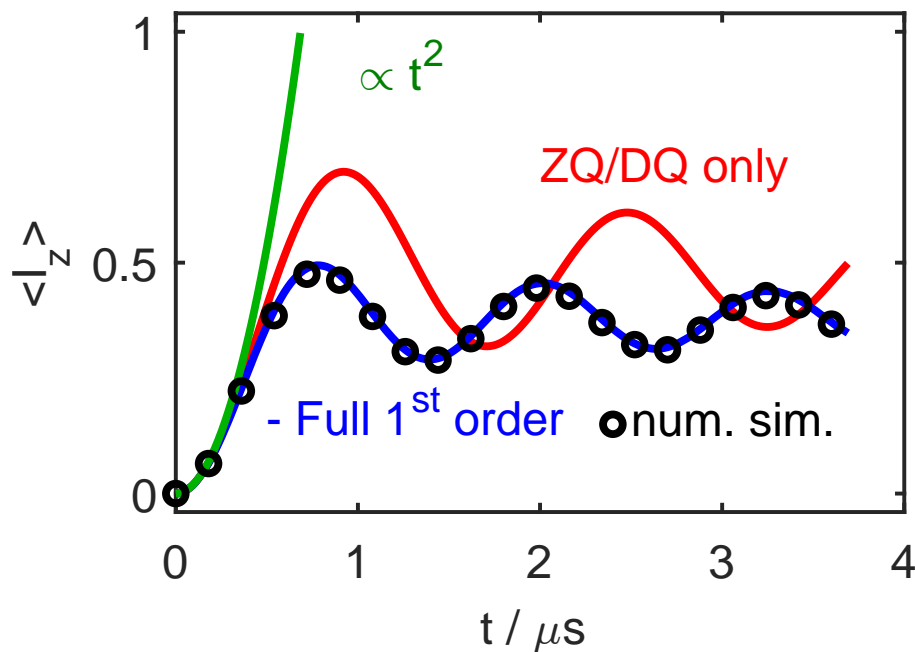


Fig. S6: Comparison of $S_z \rightarrow I_z$ polarization transfer efficiencies calculated using an effective Hamiltonian including all first order terms (blue) or only the flip-flop terms (red) with a full numerical simulation (black circles). A two-spin $e^{-1}\text{H}$ spin pair with a distance $r_{en} = 2.5 \text{ \AA}$ is used in the numerical simulations. This is a very strongly coupled proton. The green line illustrates the initial build-up

S.4 Three-spin transitions

Some small features in the Experimental DNP profiles cannot be explained by the electron-nuclear two-spin model. It is well known that there are also electron-nuclear-nuclear three-spin transitions. A comprehensive treatment for them would require second-order average Hamiltonian theory. However, the position of these features can be estimated by simply doubling the nuclear Zeeman frequency and then looking for matching conditions in exactly the same way as in the two-spin case. This is shown in Fig. S7.

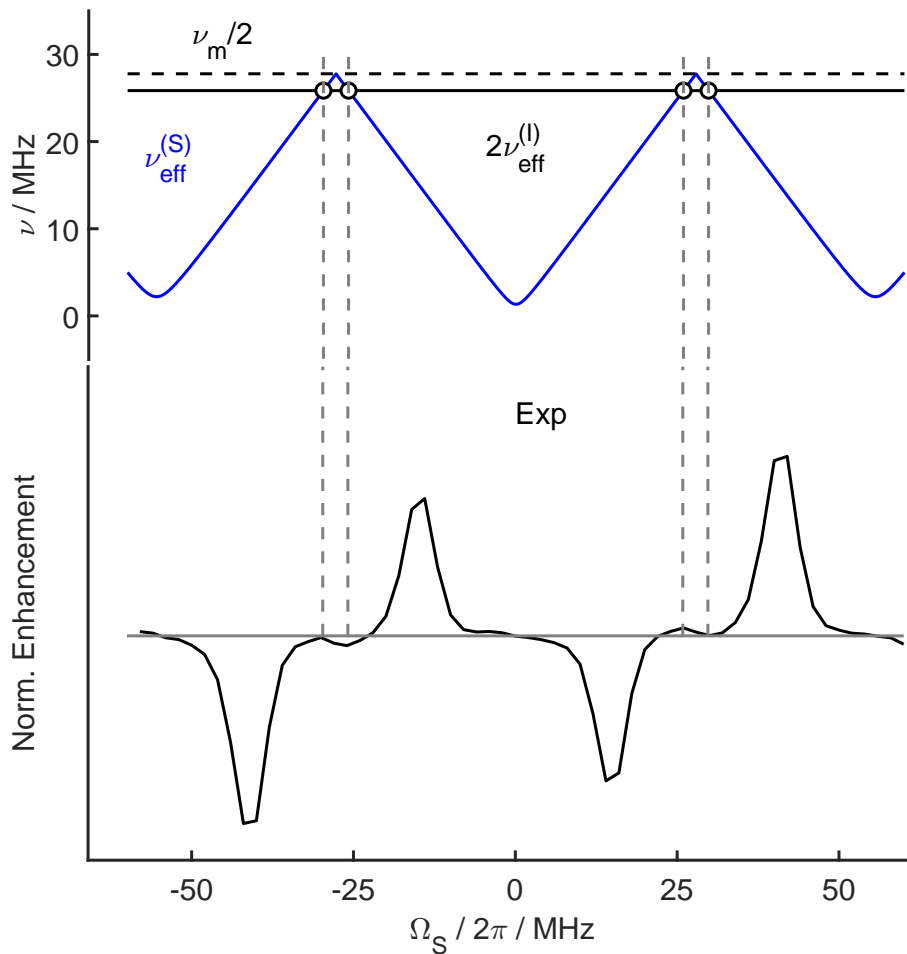


Fig. S7: Predicted offsets for three-spin transitions for XiX DNP with $t_{p,1}=12$ ns and $t_{p,2}=6$ ns.

S.5 Resonator profile

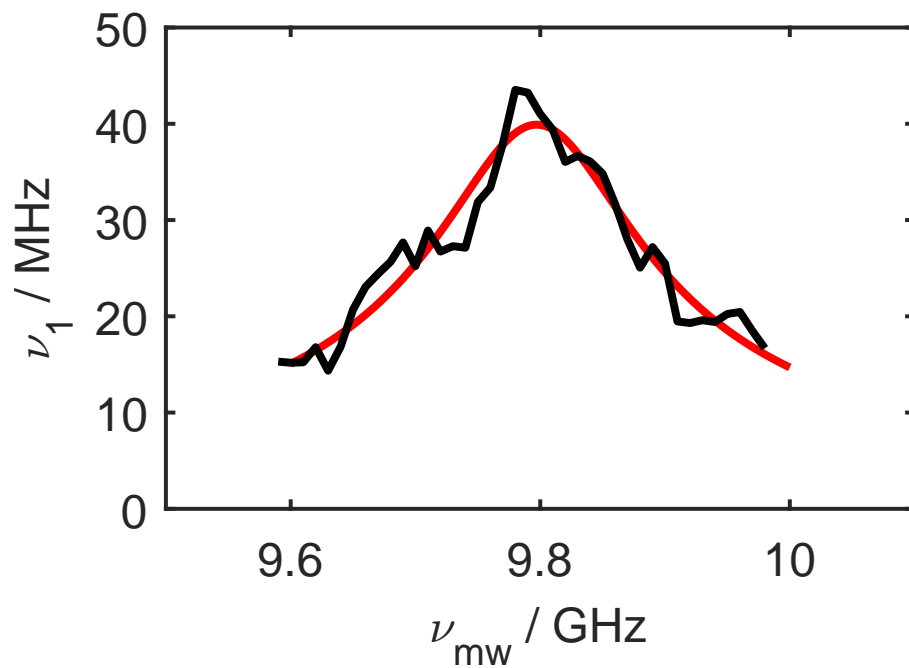


Fig. S8: Experimental resonator profile (black), determined by nutation experiments, and Lorentzian fit (red). $\nu_{1,\text{max}}=40$ MHz, $Q=61$.

S.6 Experimental determination of $T_{1,e}$

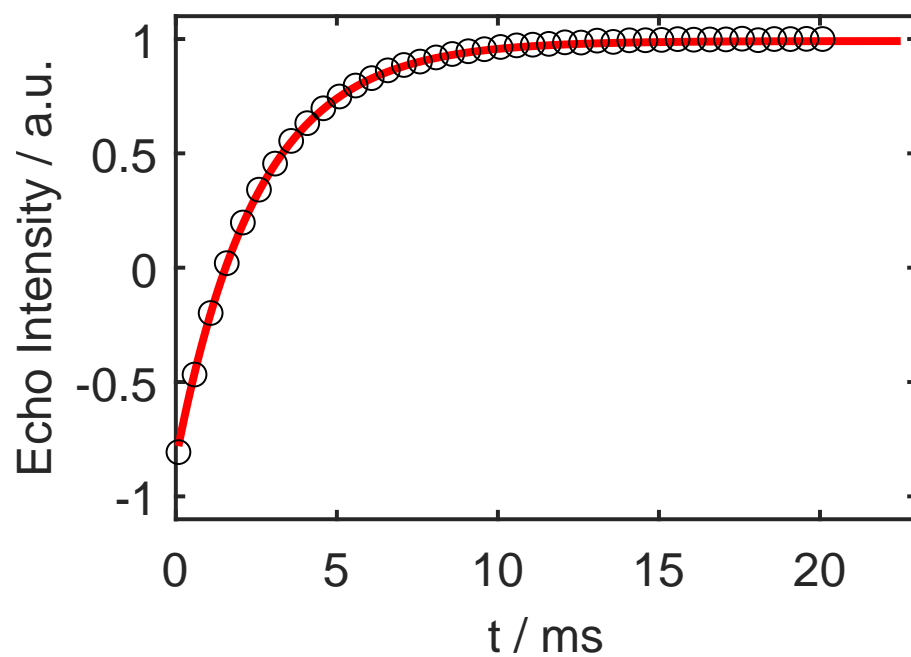


Fig. S9: Inversion recovery data for the electron spin (black circles) and exponential fit (red). $T_{1,e}=2.5$ ms

S.7 Experimental determination of $T_{1,n}$

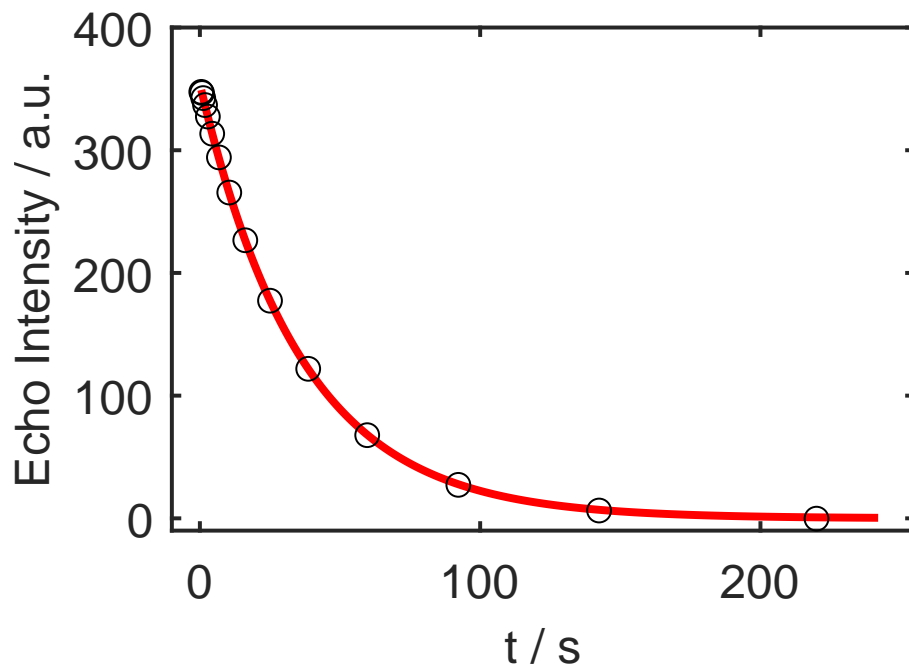


Fig. S10: Experimental proton polarization decay after 60 s of adiabatic solid effect DNP (black circles) and exponential fit (red). $T_{1,n}=36.2$ s

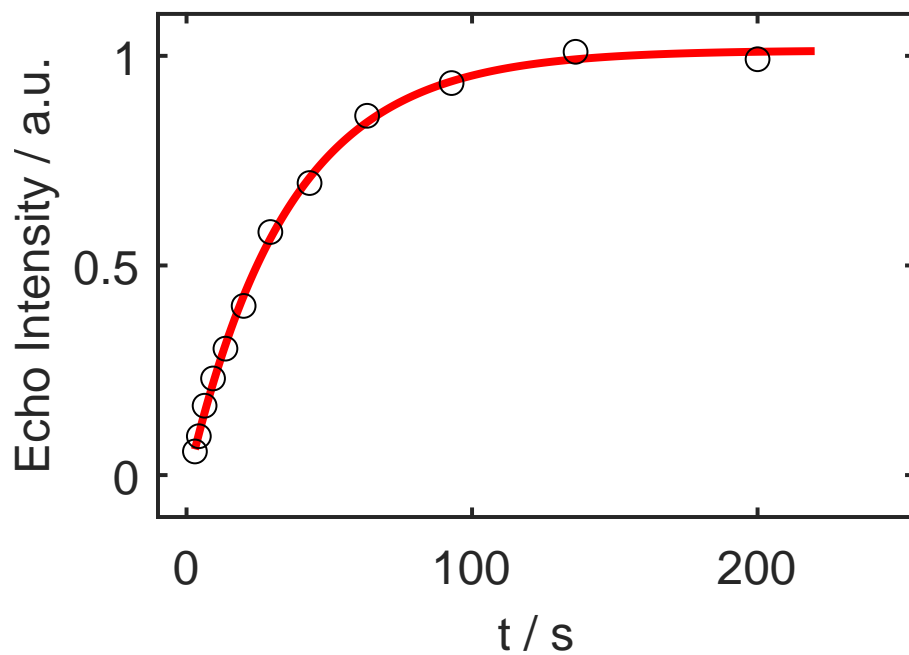


Fig. S11: Proton saturation recovery data without DNP (black circles) and exponential fit (red). $T_{1,n}=35$ s